531 DETECTION OF BOUNDARY LAYER AND ENTRAINMENT USING GROUND-BASED AEROSOL LIDAR

Virginia R. Sawyer[1]*, Zhanqing Li[1], Ellsworth J. Welton[2]
[1]University of Maryland, College Park, MD; [2]NASA-GSFC, Greenbelt, MD

1. ABSTRACT

The planetary boundary layer (PBL) and its associated entrainment zone are important features in the thermodynamic structure of the lower troposphere, but they may be easier to detect by their effect on aerosol and clouds than by thermodynamic profiling of the atmosphere. NASA's Micro-pulse Lidar Network (MPLNET) supports ground-based lidar observations at a number of sites across the globe, some of which have operated continuously for years. With an algorithm for automated PBL detection based on the backscatter gradient, this data makes it possible to observe the diurnal development and seasonal variability of the PBL height with a temporal resolution of minutes. Such information is useful for understanding aerosol transport and interaction between aerosol and the PBL.

The PBL detection algorithm combines the wavelet covariance transform approach proposed by Davis et al. (2000) and Brooks (2003) with an iterative curve-fitting process from Steyn et al. (1999). The former method provides a first guess for the latter which is adaptable to a wide range of climates and weather conditions; the latter method refines the PBL height and adds an estimate of entrainment zone depth. The combined algorithm is computationally simple enough to use operationally, while successfully identifying the backscatter features associated with the PBL. The results are months-long climatologies of PBL behavior at MPLNET sites across the globe, verifiable by radiosonde data, with estimations of the entrainment occurring between the mixed layer and free troposphere.

*Corresponding author address: Virginia R. Sawyer, Department of Atmospheric and Oceanic Science, University of Maryland, College Park, MD 20742-2425
email: vsawyer@atmos.umd.edu

2. INTRODUCTION

The PBL is the part of the troposphere that is directly affected by surface conditions, ranging from several hundred meters to a few kilometers in depth, and distinguishable from the free troposphere above it by differences in flow, thermodynamic properties, and chemical content. Strong surface heating promotes convection that can lift the boundary layer as high as 5 km even outside the tropics (Ma et al. 2011). At nightfall, or even during a solar eclipse (Amiridis et al. 2007), the PBL height collapses into a shallow stable boundary layer. Even where surface heating is weak, the PBL height changes significantly over time scales of hours.

The most direct way to detect the PBL is in the thermodynamic profile taken from radiosonde launches. Even during an intensive campaign, however, only four data points per day can be determined (Figure 1). At continental sites in the Western Hemisphere, the operational radiosonde launches at 0000 and 1200 UTC are poorly timed for PBL detection because of the rapid change in conditions during the morning and evening. In contrast, ground-based remote sensing offers temporal resolutions of minutes (Figure 2) and can collect continuous data without human intervention. Wind profiling provides some clues about the turbulence structure, so radar wind profilers and sodar are sometimes capable of detecting the PBL (Beyrich and Görsdorf 1995); another useful set of data is the relative concentration of aerosol with height. Because the PBL is buoyantly stable and thus traps most aerosol near the surface, the aerosol backscatter signal can be used as a proxy for PBL height. At a 5-minute resolution, there can be 288 data points per day—enough to resolve the diurnal development, variability, and collapse of the PBL.

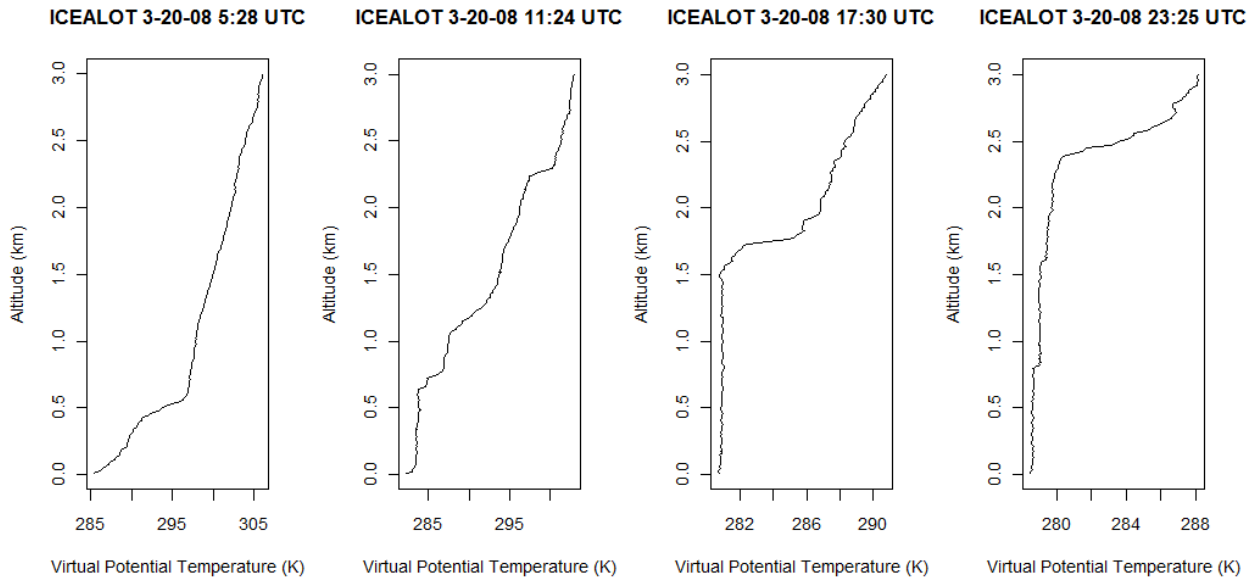

Figure 1. Virtual potential temperature profiles from a single day during the ICEALOT research campaign. Four PBL heights can be detected for the 24-hour period.

Buoyant stability prevents the mixing of aerosol through the PBL under all but a few special circumstances (Donnell et al. 2001, Twohy et al. 2002, Henne et al. 2004, Ding et al. 2009). A well-mixed boundary layer has a vertically uniform aerosol concentration that is generally more polluted than the free troposphere (Melfi et al. 1985). The free troposphere is often much more vertically stratified. These differences are visible in plots of lidar backscatter: the signal in the PBL is stronger and more uniform with altitude than the signal in the free troposphere. Boundary layer clouds, which return backscatter signal much brighter than aerosol, can also help determine the PBL (Davis et al. 2000).

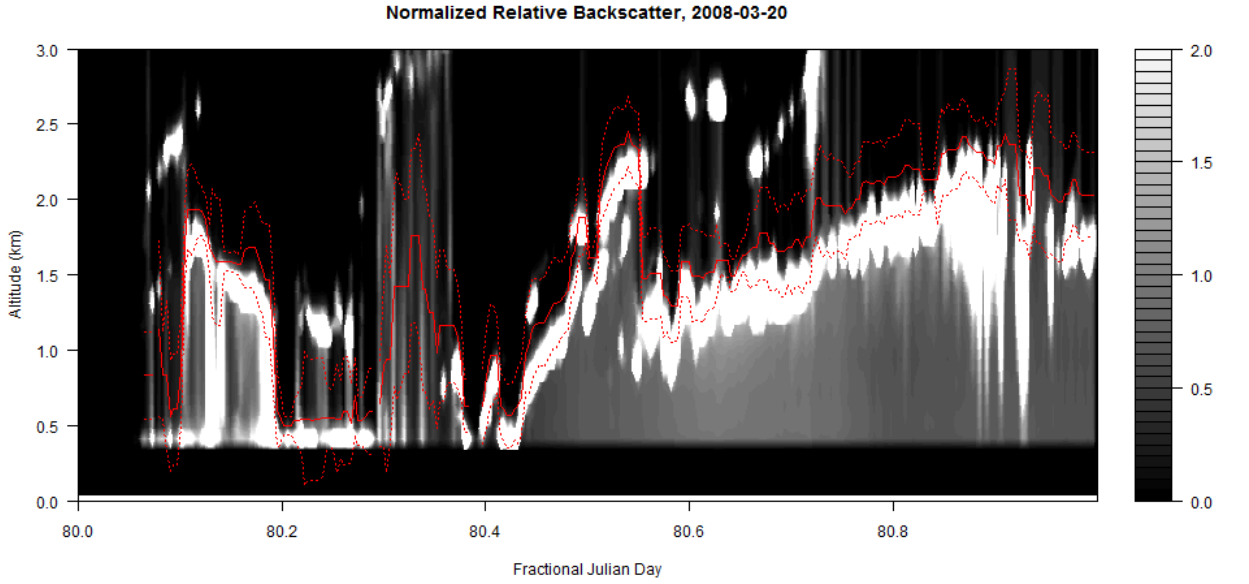

Figure 2. MPL backscatter time series from the same day during ICEALOT. Bright signals indicate cloud or precipitation; gray is aerosol. The red lines indicate detected PBL and EZD depths.

3. ICEALOT AND SGP

Two micropulse lidar (MPL) deployments served as examples to develop and validate a lidar PBL detection method. ICEALOT was a research cruise that lasted six weeks in the spring of 2008, its focus the Arctic haze responsible for peak aerosol concentrations in the region every spring. The MPL aboard the *R/V Knorr* was part of the NASA's MPLNET program. Over Gulf Stream waters in the far north (Figure 3), the diurnal cycle of the PBL is weak to nonexistent. Multiple stable layers in the lower troposphere were common due to the warm conveyor belt and other transport processes.

ARM's Southern Great Plains site in Oklahoma (36°36'18.0" N, 97°29'6.0" W) experienced more typical continental PBL processes, and its MPL instrument was deployed much longer: data is available from 1996 to 2004. In both cases, radiosonde launches took place four times per day at the same location as the lidar. For the SGP site, a radiosonde-based PBL product has already been developed; the results of Liu and Liang (2010) are used for comparison here. Although there is considerable uncertainty in radiosonde-derived PBL height data, this makes it possible to evaluate lidar-derived PBL heights against independent observations.

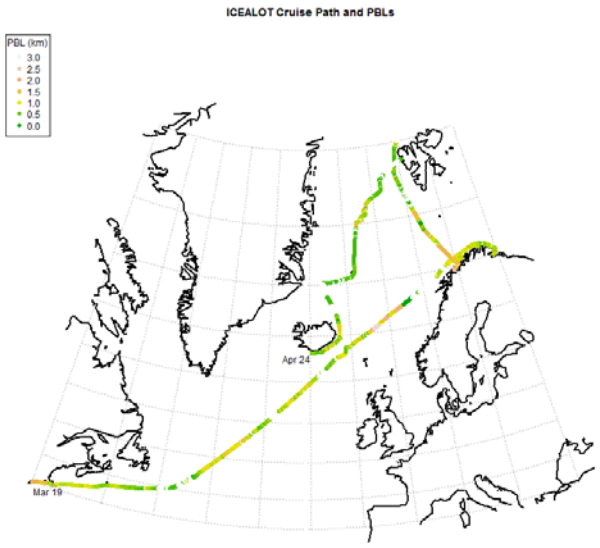

Figure 3. The path of the ICEALOT cruise and the lidar-derived PBL heights by location.

4. BACKSCATTER GRADIENT METHODS

Simple gradient methods for PBL detection involve setting threshold values for mixed-layer backscatter (Melfi et al. 1985, Palm et al. 1998) or taking the first derivative of the backscatter signal (Amiridis et al. 2007). These are effective for short-term, relatively uniform data sets, but they require too much prior knowledge of the instrument properties and atmospheric conditions to be suitable for automation. Edge detection software in programs such as Photoshop may also be capable of layer detection in lidar backscatter (Parikh and Parikh 2002). But two more sophisticated algorithms based on the backscatter threshold concept are widely used.

Two prominent PBL detection methods rely on the sharp negative gradient in aerosol backscatter that typically occurs at the PBL top. The wavelet covariance transform (Davis et al. 2000, Brooks 2003) is suitable for automated PBL detection because of its speed and the lack of prior knowledge required to use it effectively. For a backscatter profile $f(z)$, step translation b and arbitrarily-assigned dilation a (1 km), the Haar wavelet covariance

$$\left(\frac{z-b}{a}\right) = \begin{cases} -1: & b - \frac{a}{2} \le z \le b \\ 1: & b \le z \le b + \frac{a}{2} \\ 0: & elsewhere \end{cases}$$

and

$$W_f(a,b) = a^{-1} \int_{zb}^{zt} f(z) h\left(\frac{z-b}{a}\right) dz$$

defines a candidate PBL height as the altitude b of the maximum value of $W_f(a,b)$. In other words, the Haar function most closely resembles the backscatter sounding when its step occurs at the altitude of maximum wavelet covariance.

A separate method developed by Steyn et al. (1999) and Hägeli et al. (2000) is more sensitive than the wavelet covariance transform to small-scale changes in the PBL height. It is also less likely to err when the profile contains bright non-boundary signals such as cirrus clouds or elevated aerosol

layers. However, because the method involves a curve-fitting algorithm that relies on a reasonable initial guess, it is not suited for automated PBL detection.

Combining the two methods can result in a single algorithm retaining the advantages of both. The wavelet covariance transform is used to find a first guess PBL solution for the curve-fitting algorithm from Steyn et al. (1999), which simultaneously refines the PBL height and determines the depth of the entrainment zone (EZD). The curve-fitting routine uses an idealized profile

$$B(z) = \frac{(B_m + B_u)}{2} - \frac{(B_m - B_u)}{2}\,\mathrm{erf}\left(\frac{z - z_m}{s}\right)$$

in which B_m and B_u are the mean backscatter of the mixed layer and lower troposphere, respectively, and z_m is the wavelet-derived PBL top height. The variable s defines the depth of the error function and is proportional to the EZD (assumed equal to a for the initial value). The RMSD between this idealized profile and the actual backscatter sounding is then minimized by simulated annealing (Press et al. 1992). While simulated annealing is more robust than downhill simplex iteration where local minima and troughs may occur in the solution space, it introduces an element of randomness that must be smoothed out in the final step of the algorithm. Hägeli et al. (2000) proposed a running-mean filter with an interval appropriate to the scales involved. An example backscatter profile, wavelet covariance transform, and iterated solution are shown in Figure 4.

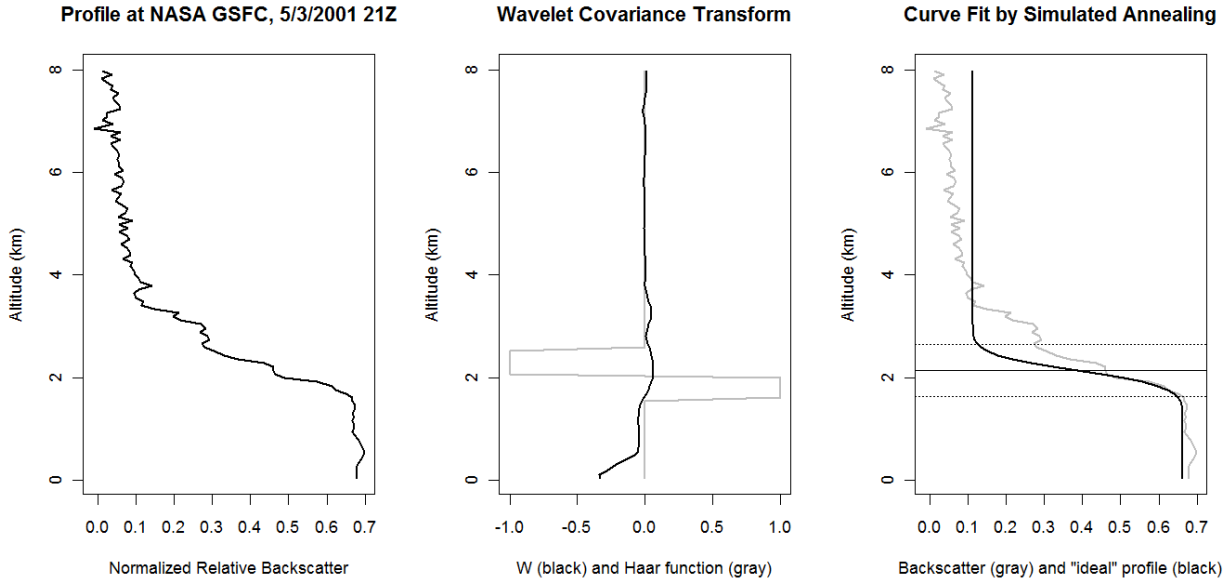

Figure 4. Example lidar backscatter profile, the corresponding wavelet covariance transform with the Haar function at b set to maximize $W_f(a,b)$, and the final profile fitted by simulated annealing.

5. EVALUATION

MPL uses a relatively powerful laser that achieves eye safety at the expense of accurate retrievals in the lowest 400 m of the atmosphere. The range limitations of the lidar make it especially difficult to detect shallow, stable boundary layers, which occur mainly at night (Figure 5). It is crucial to consider the stability of the lower troposphere when evaluating PBL results, regardless of the instrument that was used for detection. In addition to the range limits of the lidar, the typically deeper inversions of stable boundary layers have less dramatic gradients in potential temperature and aerosol content than the sharper convective boundary layers. Aerosol plumes do not necessarily follow the collapse of the PBL at nightfall, but often

remain near the altitude of the maximum daytime PBL top in elevated residual layers.

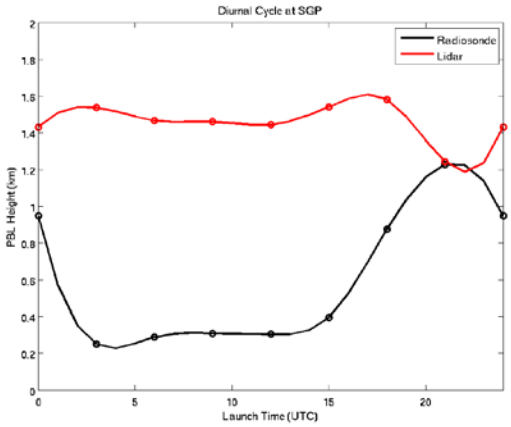

Figure 5. Diurnal cycle of the PBL at SGP, compared between Liu and Liang (2010) radiosonde PBLs (black) and lidar-derived PBLs at times chosen to match sonde launches (red).

For ICEALOT, where the time series was short enough that potential temperature soundings could be analyzed by hand to detect both the PBL and any residual layer, it can be shown that when the true PBL fell below the range limit of the MPL, the combined algorithm detected a residual layer instead (Figure 6). There are relatively few such cases because the ICEALOT data represents marine boundary layers over a sea surface that remained significantly warmer than the air temperature. At SGP, a continental site with a strong diurnal cycle in surface heating, most stable boundary layers fell below the limit. No relation was found between them and the lidar-derived PBL heights.

For neutral and convective cases, a moderate correspondence (R^2 ~ 50%) exists between the radiosonde-derived PBL heights and the lidar-derived values (Figure 7). Detection algorithms for both instruments show considerable uncertainty. The signal of low cloud bases, multiple layers, and rapidly-changing conditions during morning and evening launch times may confuse either scheme. Additional instruments such as lower-powered ceilometers may complement the range, while remote sensing of temperature profiles may shed further light on the situation.

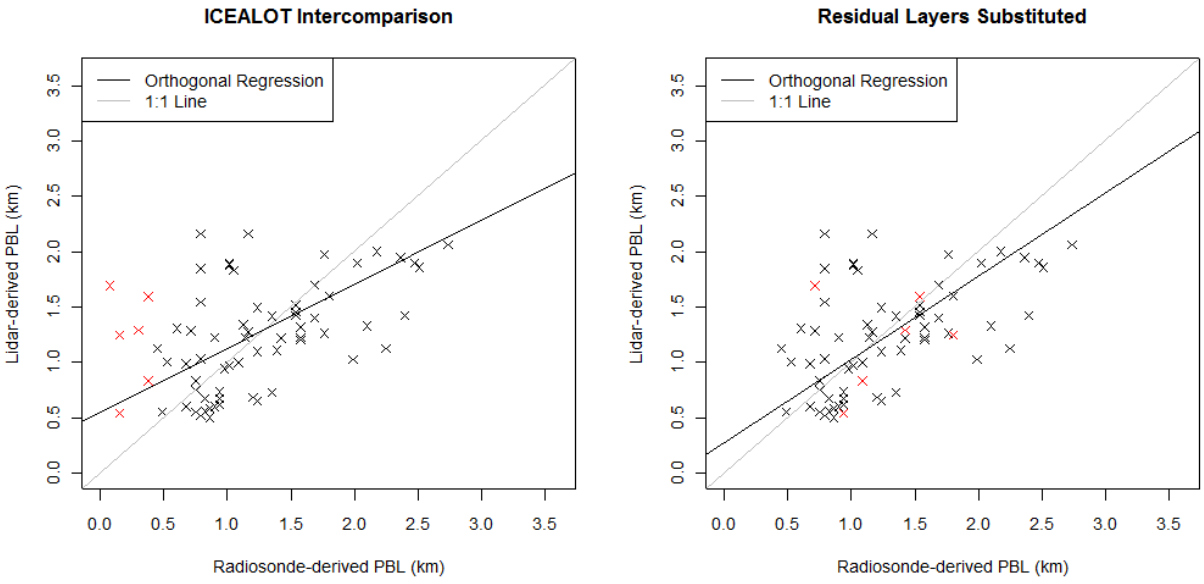

Figure 6. Comparison between radiosonde-derived and lidar-derived PBL heights during the ICEALOT campaign. In the first figure, radiosonde-derived PBL heights below 400 m are marked in red; in the second, residual layers detected using radiosonde data are substituted for PBL heights and compared again to the lidar-derived PBLs. The results are much closer to the 1:1 line.

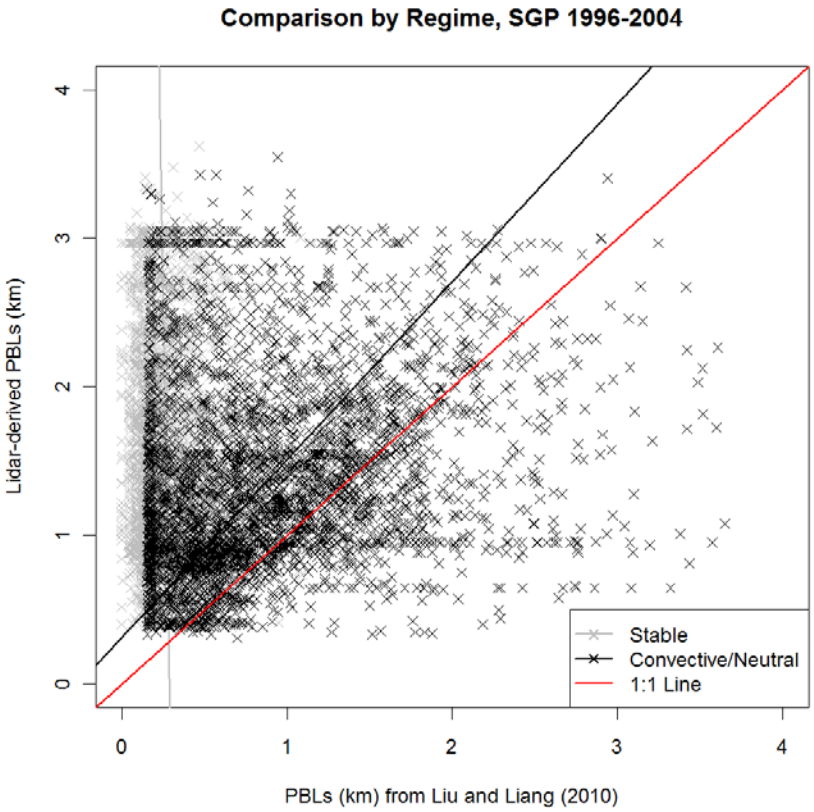

Figure 7. Comparison between radiosonde-derived and lidar-derived PBL heights from the SGP site. PBL heights classed as stable by Liu and Liang (2010), in gray, are considered separately. The orthogonal regression of neutral and convective cases is close to the 1:1 line.

6. DISCUSSION

By combining a wavelet covariance transform with simulated annealing, the PBL detection algorithm retains the advantages of both methods: it is adapted to the needs of automated PBL detection but somewhat more sensitive than the pure wavelet covariance algorithm to small-scale changes in PBL height. By using ground-based remote sensing rather than the more straightforward radiosonde data, the algorithm is able to greatly improve the temporal resolution of PBL height retrievals. For data from the ICEALOT research cruise (North Atlantic) and from the ARM SGP site (Oklahoma), the algorithm was used to detect PBL heights in MPL retrievals and then compared against PBL heights detected in the radiosonde-derived profiles of potential temperature with altitude.

R^2 values of approximately 50% are usual for orthogonal regressions between radiosonde-derived PBL heights and lidar-derived PBL heights taken from times matched to radiosonde launch periods. The correspondence between the instruments varies by the stability regime of the lower atmosphere, which at the SGP site is part of a strong diurnal cycle. Stable nocturnal boundary layers often fall below the minimum height range detectable by MPL. For ICEALOT, it was clear that in such cases the lidar algorithm detected elevated residual layers instead. Considerable uncertainty exists in PBL detection by either instrument, with possible interference due to the behavior of clouds or a mismatch between the thermodynamic profile and the aerosol structure. Additional instruments, such as low-powered lidar used to complement MPL backscatter or the remote sensing of thermodynamic properties, may improve PBL detection at SGP and other sites.

7. ACKNOWLEDGEMENTS

This work relied on the help of Connor Flynn, Shuyan Liu and Xin-Zhong Liang for their work with the SGP data; the ICEALOT scientists and the crew of the *R/V Knorr;* MPLNET at NASA-GSFC; and Jianjun Liu.

REFERENCES

Akimoto, H., 2003. Global air quality and pollution. *Science* 302, 1716-1719.

Amiridis, V., et al., 2007. Aerosol lidar observations and model calculations of the planetary boundary layer evolution over Greece, during the March 2006 total solar eclipse. *Atmos. Chem. Phys*., 7, 6181–6189.

Beyrich, F. and U. Görsdorf, 1995. Composing the diurnal cycle of mixing height from simultaneous sodar and wind profiler measurements. *Bound.-Layer Meteor.* 76, 387-394.

Brooks, Ian M., 2003. Finding boundary layer top: application of a wavelet covariance transform to lidar backscatter profiles. *J. Atmos. Oceanic Technol.* 20, 1092-1105.

Davis, K. J., et al., 2000. An objective method for deriving atmospheric structure from airborne lidar observations. *J. Atmos. Oceanic Technol.* 17, 1455-1468.

Ding, A., et al., 2009. Transport of north China air pollution by midlatitude cyclones: Case study of aircraft measurements in summer 2007. *J. Geophys. Res.* 114, D08304.

Donnell, E.A., D.J. Fish and E.M. Dicks, 2001. Mechanisms for pollutant transport between the boundary layer and the free troposphere. *J. Geophys. Res.* 106, 7847-7856.

Georgoulias, A.K., et al., 2009. Statistical analysis of boundary layer heights in a suburban environment. *Meteorol. Atmos. Phys.* 104, 103-111.

Hägeli, P., D.G. Steyn and K.B. Strawbridge, 2000. Spatial and temporal variability of mixed-layer depth and entrainment zone thickness. *Boundary-Layer Meteorol.* 97, 47-71.

Henne, S., et al., 2004. Quantification of topographic venting of boundary layer air to the free troposphere. *Atmos. Chem. Phys.*, 4, 497–509.

Hennemuth, B. and A. Lammert, 2006. Determination of the atmospheric boundary layer height from radiosonde and lidar backscatter. *Boundary-Layer Meteorol*. 120, 181-200.

Ma, M., et al., 2011. Characteristics and numerical simulations of extremely large atmospheric boundary-layer heights over an arid region in north-west China. *Boundary-Layer Meteorol.* DOI 10.1007/s10546-011-9608-2.

Liu, S. and X.-Z. Liang, 2010. Observed diurnal cycle climatology of planetary boundary layer height. *J. Climate* 23, 5790-5809.

Melfi, S.H., et al., 1985. Lidar observations of vertically organized convection in the planetary boundary layer over the ocean. *J. Climate Appl. Meteor.* 24, 806-821.

Palm, S., et al., 1998. Inference of marine atmospheric boundary layer moisture and temperature structure using airborne lidar and infrared radiometer data. *J. Appl. Meteor.* 37, 308-324.

Parikh, N.C. and J.A. Parikh, 2002. Systematic tracking of boundary layer aerosols with laser radar. *Optics & Laser Technology* 34: 177-185.

Press, W. H., S. A. Teukolsky, W. T. Vettering, and B. R. Flannery, 1992. *Numerical Recipes in FORTRAN: The Art of Scientific Computing.* 2d ed. Cambridge University Press, pp. 436-447.

Seibert, P., et al., 2000. Review and intercomparison of operational methods for

the determination of the mixing height. *Atmos. Environ.* 34, 1001-1027.

Seinfeld, John H. and Spyros N. Pandis. *Atmospheric Chemistry and Physics: from Air Pollution to Climate Change*. 2nd ed. Hoboken, NJ: Wiley, 2006.

Steyn, D.G., M. Baldi and R.M. Hoff, 1999. The detection of mixed layer depth and entrainment zone thickness from lidar backscatter profiles. *J. Atmos. Ocean. Technol.* 16, 953-959.

Stull, Ronald B, 1988. *An Introduction to Boundary Layer Meteorology.* Kluwer Academic Publishers, 666 pp.

Twohy, C.H., et al., 2002. Deep convection as a source of new particles in the midlatitude upper troposphere. *J. Geophys. Res.* 107, D21, 4560.